Arboriculture & Urban Forestry 2022. 48(4):217–232
https://doi.org/10.48044/jauf.2022.016

Quantitative Tools for the Prediction of Pavement Damages Associated with Urban Trees

By Louis S.H. Lee

Abstract. Background: Tree pits are urban green infrastructures in paved areas. But tree roots and flares, especially of larger trees, may come into conflict with pavement, resulting in tree health decline and repair costs. This study aimed to (1) establish allometric relationships between diameter at breast height (DBH) and trunk flare diameter (TFD) of common urban tree species, and (2) identify factors affecting the presence and magnitude of protruding roots and flares. Methods: The terms "protruding roots" and "protruding flares" were strictly defined as roots and flares reaching or exceeding the border between the open soil and the adjacent paving material. The study surveyed 1,100 trees of 14 species planted in tree pits in Chai Wan, Hong Kong. Results: DBH was a significant predictor of TFD but was less significant when trees with protruding roots or flares were considered separately. In most logistic models, DBH was significantly and positively related to the odds ratio of the occurrence of protruding roots and flares. Overall, a centimetre increase in DBH brought 1.049 to 1.114 times higher likelihood of protruding roots and flares. Multiple regression suggested that for every square-metre increase in the open soil area in tree pits, the maximum length of protruding roots and flares increased by 0.154 to 0.172 m. This relationship could be attributed to the underlying association between DBH and open soil area. Species-specific regression results were tabulated to allow more accurate estimation of protruding roots and flares. Conclusion: For urban planners and pavement engineers, the approach recommended in this study could be adopted to optimise urban greening and pavement design.

Keywords. Pavement Damage; Protruding Roots; Tree Care; Tree Pit; Trunk Flare; Urban Green Infrastructure.

INTRODUCTION

Trees serve as a nature-based solution to challenges related to sustainability. Urban densification, to a certain extent, has fuelled land-use competition. Urban space allocation for walking and greening has been optimised by the use of tree pits. Paved areas could impact surface warming (Zheng et al. 2014), hydrological balance (Timm et al. 2018), and vegetation survival (Chen et al. 2017). In urban areas, trees aid thermal regulation (Cheung and Jim 2018), thermal comfort improvement (Lee et al. 2020), stormwater retention (Bartens et al. 2009), acoustic insulation (Ozer et al. 2008), air purification (Islam et al. 2012), biodiversity reconciliation (O'Sullivan et al. 2017), and landscape beautification (Lee et al. 2021). Such benefits are maximised as trees mature. Yet older and larger trees may be damaging to other urban infrastructures (Rotherham 2010). The costs and benefits of greening could be estimated more accurately using results from detailed dendrometric analysis of urban trees.

Large-stature trees in tree pits may damage pavement surface. An extensive and large root system may cause subsidence, cracks, displacements, and spalling (Watson et al. 2014; Mullaney et al. 2015; Giuliani et al. 2017; Li and Guo 2017; Loprencipe and Pantuso 2017; Grabosky and Gucunski 2019; Johnson et al. 2019). Roots may grow towards areas with higher oxygen and moisture concentration (Barker and Peper 1995; D'Amato et al. 2002; Morgenroth and Buchan 2009; Lucke and Beecham 2019). The permeability of and soil volume under pavement would affect root growth. Under permeable pavement, moisture in free-draining soil pores could encourage vertical and lateral root growth (Stovin et al. 2008; Bartens et al. 2009; Grabosky et al. 2009; Ow and Ghosh 2017; Ebrahimian et al. 2018). Fissures among bricks used

for pavement may allow some degree of soil moisture replenishment, whereas the surface runoff on concrete surfaces would be lost to the urban drainage system. Therefore, characterising the habitat conditions by the dimensions and type of pavement is vital.

Without appropriate care, pavement may interfere with root growth. In the literature, belowground root expansion was detected and predicted with various approaches, such as statistical modelling (Johnson et al. 2019), numerical analysis (Giuliani et al. 2017; Li and Guo 2017), mechanical analysis (Grabosky and Gucunski 2019), and ground-penetrating radar (Krainyukov and Lyaksa 2016; Altdorff et al. 2019). But, in frontline operations, a site manager often needs to take care of a large number of trees. Simple and replicable methods could raise the efficiency of tree inspection. For researchers, with a considerably large sample generated from tree survey, reliable allometric relationships could be drawn via statistical means.

Flares stemming from a trunk tapering near the ground can be quantified by trunk flare diameter (TFD), which is predictable by diameter at breast height (DBH). In order to avoid pavement damage, minimal open soil surface area could be determined according to predicted TFD values (North et al. 2015; Hilbert et al. 2020). Hilbert et al. (2020) also regressed the occurrence of pavement damage on dendrometric and habitat variables. However, in their model, the classification of possible damages was lacking. The central tenet of prediction models was the higher likelihood of damage with larger TFD. Yet confounding factors (such as the geometrical shape of trunk flare) added complexities to the damage prevention through TFD prediction. Holding TFD constant, flares reaching laterally towards a corner of a tree pit, instead of a side, have more room for extension before inflicting damage. A more-direct indicator is desperately needed. Emphasis should be placed on flares and roots which are longer and larger, providing higher concern over their potential to inflict damage. Therefore, a more direct, quantitative variable could be utilised in order to characterise the potential conflict between pavement and trees.

A narrow selection of tree species from a few genera were covered in previous studies on pavement damage in relation to trees. Some examples are *Acer*, *Fraxinus*, *Gleditsia*, *Koelreuteria*, *Melaleuca*, *Platanus*, *Populus*, *Pyrus*, *Quercus*, and *Zelkova* (D'Amato et al. 2002; Blunt 2008; Smiley 2008; Gilman and Grabosky 2011; North et al. 2015; Grabosky and Bassuk 2016; Johnson et al. 2019; Lucke and Beecham 2019). A wider range of tree species for urban greening should be examined. Growth behaviour of trees is species-specific, so the allometric models should be as well (Semenzato et al. 2011; Marziliano et al. 2013; Oldfield et al. 2015; Benson et al. 2019b). Non-conspecific allometric equations should be carefully and never indiscriminately applied. Previously, no attempts at allometric modelling were conducted on samples entirely consisting of trees which were in possible conflict with pavement. Therefore, more urban tree species could serve as potential samples for the present research.

In Hong Kong, pavement damages have been observed around trees whose roots or flares have reached or breached the edge of the open soil surface of a tree pit. Such roots or flares are visually detectable by inspecting the interface between open soil and pavement material. The specific terms, namely, protruding roots or protruding flares, are defined in the Materials and Methods section. The aims of this research are to (1) establish allometric relationships between DBH and TFD of common urban tree species and (2) identify factors affecting the presence and magnitude of protruding roots and flares. Practical recommendations for urban greening and infrastructure management are distilled from the findings.

MATERIALS AND METHODS

Study Location

This research was conducted in Hong Kong, China (22.3° N, 114.2° E). Approximately 24.9% of the 1,100 km^2 land area was classified as built-up land (Planning Department 2020). The population size of 7.34 million are packed into limited-development areas due to the hilly terrain (Census and Statistics Department 2018). The resulting high building density leaves very little space for street-level greening. Nevertheless, from 2010 to 2020, approximately 544,300 trees were planted in urban areas (Greening, Landscape & Tree Management Section Development Bureau 2021). Even in paved areas, trees are planted for landscaping purposes. Transport land use occupies 46 km^2 of land surface, where tree pits dot the pavements along many roads.

With a rationale of preventing pavement damage around tree pits, this empirical study focused on trees growing in tree pits in Chai Wan, Eastern District,

Hong Kong. A 1.811 km^2 area, which excluded peri-urban rural fringes, contained 31 roads and streets featuring tree pits, adding up to a total length of 14.21 km. Under development since the 1950s, the study location featured both mature trees as well as new plantings in freshly laid pavements. Completely decomposed granite, with haphazard application of organic amendments, was commonly used as the backfill soil in Hong Kong. Comparable development patterns still apply to other parts of Hong Kong. The findings could be transferred to neighbouring biogeographical zones.

Tree Survey and Collected Variables

A tree survey was conducted from 2020 December 16th to 2021 January 28th. During the tree survey, each tree served as an individual sampling unit (Figure 1). Dendrometric variables were recorded. DBH was measured at a height of 1.3 m from the soil surface. TFD was measured in a similar fashion to North et al. (2015). In order to measure the TFD of a tree, the outer tips of each flare were first marked at soil level. Then, a measurement tape was used to connect all marked tips, measuring the trunk flare circumference which was divided by π to obtain TFD. Height (H) was estimated from soil surface to tree top. The lean angle of the main trunk was determined at a height of 1.3 m. For trees with aerial roots, only the central trunk was measured.

Habitat factors related to tree pits were recorded as in Figure 1. Open soil surface area in tree pits was

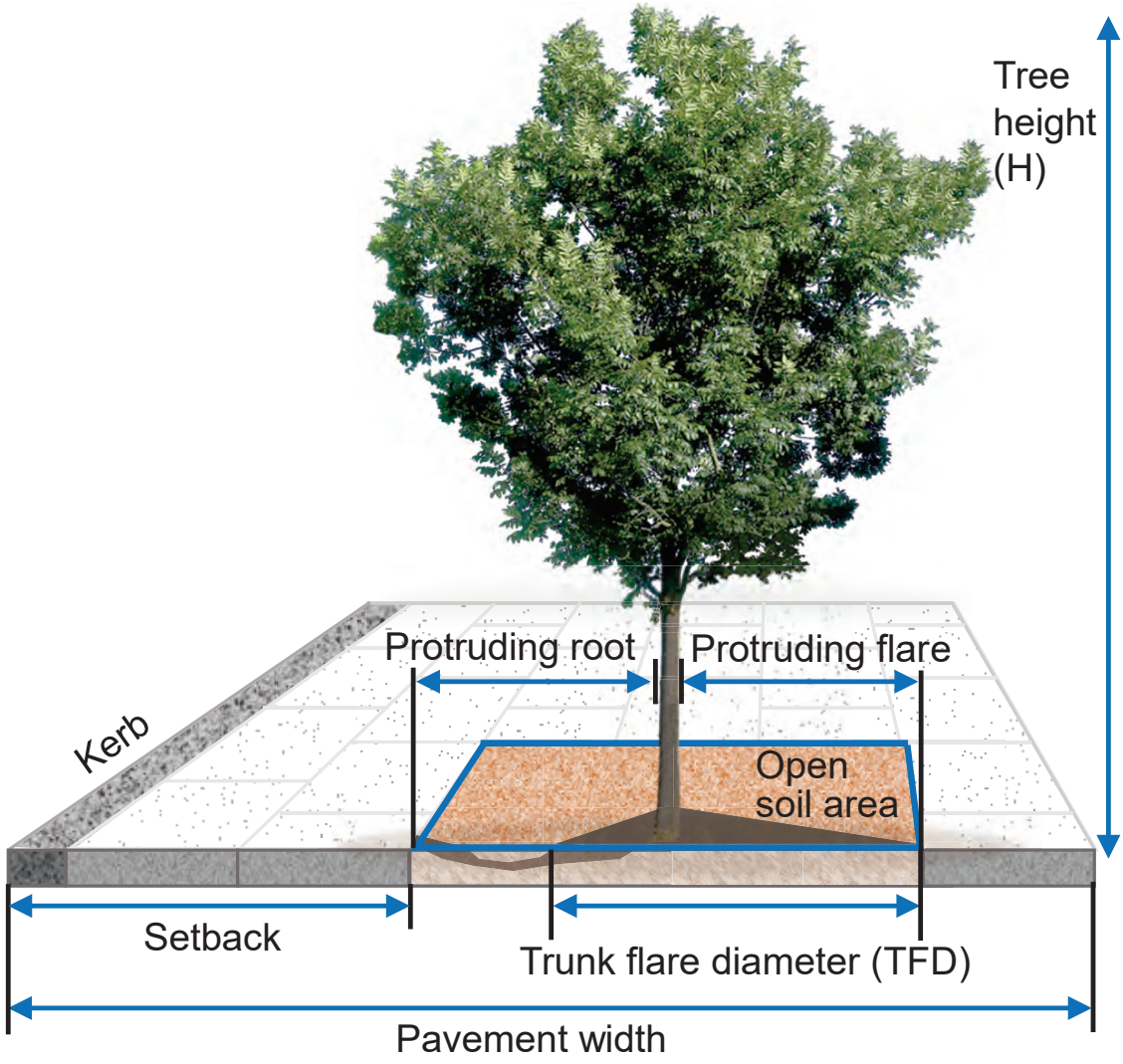

Figure 1. Illustration of dendrometric and habitat factors measured in this study. Except for open soil area which was measured in square metres, all dimensional variables were measured in metres.

computed from the pits' length and width. Starting from the kerb to the opposite end, pavement width was measured perpendicular to the longitude of the pavement. Setback was measured from the kerbside edge to the proximal border of the open soil. Pavement material was dichotomously classified as brick or concrete. In the regression models, brick and concrete were given integer codes of 1 and 2, respectively.

In this study, *protruding flare* or *protruding root* indicated potential conflicts between a tree and the surrounding pavement. The description, *protruding*, implied the reaching or exceeding of the border between the open soil and the adjacent paving material. Being connected to the tree under the ground, a *protruding root* extended outward in the soil and reached the surface at a distance from the root collar (Figure 2a). Such connection, unless unearthed, remained invisible. A *protruding flare* was a trunk flare with visible connection to the main stem above soil level (Figure 2b). Protruding flares and roots were visually detected and identified. Lexically, *protruding* was used because flares or roots appeared as extending from the stem, heading outward, thereby possibly encroaching on paving materials.

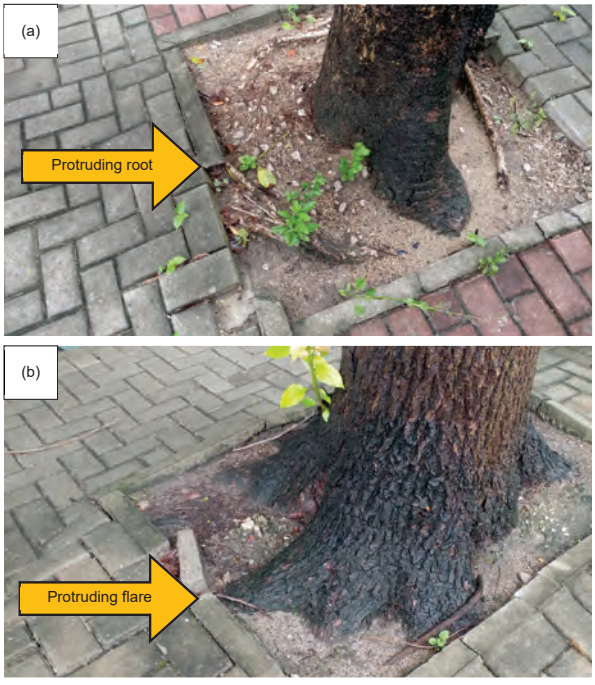

Figure 2. Presence of (a) protruding root and (b) protruding flare indicated by yellow arrows. The protruding parts were visually detectable by woody tissues reaching the border between the open soil area and paving materials.

Protruding roots or flares would imply potential stress on the root system and pavement materials. In the tree survey, the sides and corners of every tree pit were inspected. A vertical line was projected upward from the outermost tip of the protruding part. Then, the length of the protruding root or flare was determined as the linear distance from the projected line to the trunk at a height of 1.3 m (Figure 1). For this study, if multiple protruding parts were spotted, only the longest one was recorded. Thus, the maximum length was the variable of interest.

The data analysis for this study featured 3 scenarios:

- Protruding roots only: a subsample of trees featuring protruding root(s)
- Protruding flares only: a subsample of trees featuring protruding flare(s)
- Protruding roots and/or flares: a subsample of trees featuring protruding root(s) and/or flare(s)

The demarcation of the data analyses into 3 related but different scenarios was justified by the different growth behaviour of the trees. Focusing on a specific protruding part would affect the explanatory power of prediction models. For concise communication, the term *protrusion* meant a situation when protruding roots or flares, or a combination of both, were present. Also, the phrase *protruding part(s)* referred to the part(s) of the tree which was confirmed as being *protruding*.

Data Selection and Analysis

In the tree survey, 1,466 trees of 61 species were registered. All statistical tests were administered at species level and at $\alpha = 0.05$. Shapiro-Wilk tests indicated frequent deviation from normality in many data subsets. For normal approximation, only species with $n > 30$ were retained (Mann 2007). Ultimately, 1,100 trees of 14 species were selected for further analysis. Descriptive statistics of the essential dendrometric and habitat variables were presented. Using tree species as a fixed factor, Games-Howell post-hoc comparisons were conducted to group the mean values into homogeneous subsets. Due to skewness, median values were also provided.

Simple linear regression was conducted to predict TFD using DBH. Separate models were constructed for each species. Then, the usefulness of DBH in the prediction of TFD was investigated under the presence of protrusion by a separate set of regression models in which only trees with protruding roots and/or flares

were included. Five species were dropped due to insufficient sample size for reliable prediction equation (Keith 2019). To enhance the comprehensiveness of the results, error terms and confidence intervals of the regression coefficients were reported.

Binary logistic regression was administered to predict the presence of protruding parts. The 3 aforementioned scenarios, namely (1) protruding roots, (2) protruding flares, and (3) protruding roots and/or flares, were adopted. DBH, H, and lean angle functioned as dendrometric factors, whereas pavement width, open soil area, setback, and pavement material were classified as habitat factors. Following Hilbert et al. (2020), the unit of measure used for DBH was centimetres, so that odds ratio values could be more easily interpreted. Model statistics (X^2), pseudo R^2, and prediction accuracy values (Yes% and No%) were presented, followed by the effect of each factor on the odds ratio of the 3 scenarios. General models containing all 1,100 trees as well as species-specific models were presented.

Finally, multiple regression was conducted to predict the magnitude of protrusion in the 3 scenarios. The magnitude of protrusion was synonymous to the length of the protruding part under investigation in the respective scenario. Again, the same set of dendrometric and habitat factors served as predictors. The model statistics and regression coefficients of all predictors were reported. Due to the method of measurement, longer protruding roots and/or flares led to larger TFD. As a result, TFD was removed from the multiple regression models. The length of protruding roots and flares was a more-direct indicator of potential conflicts between trees and pavement, thus receiving emphasis in the prediction models. Similar to the logistic regression, both general and species-specific models were constructed.

RESULTS

Overview of Dendrometric Factors

Among large-tree species, the species rankings of DBH and TFD showed similarities (Table 1a). *Ficus altissima* featured the largest mean DBH (0.754 m), significantly exceeding the congeneric *F. microcarpa* (0.467 m). Similarly, in terms of TFD, 3 species showed a statistically distinct, descending rank: *F. altissima* (2.504 m) > *F. microcarpa* (1.797 m) > *Delonix regia* (0.956 m).

For intermediate species, DBH and TFD showed differences in the ranking with respect to tree species. A clearly delineated group with intermediate TFD values (0.501 to 0.653 m) consisted of species such as *Aleurites moluccanus* and *Bombax ceiba* (Table 1a). However, DBH distributions of intermediate species displayed complicated statistical grouping. For example, *A. moluccanus* belonged to 3 homogeneous groups.

Even more complicated grouping was observed in H (Table 1a). For instance, *Casuarina equisetifolia*, whose mean H reached 13.45 m, was significantly taller than all other species except *F. microcarpa* (11.94 m). Meanwhile, the latter was statistically comparable to upright species such as *A. moluccanus*. Complex distribution patterns also existed in the case of lean angle. Therefore, species-specific patterns in dendrometric distributions would justify further analyses at species level.

Overview of Habitat Factors

Casuarina equisetifolia and *F. altissima*, with respective mean pavement width of 9.168 m and 7.277 m, were planted in significantly wider pavements (Table 1b). Much narrower pavements were observed for the rest of the species with mean width from 3.177 to 5.967 m. Except *Lagerstroemia speciosa*, all species had notably more samples along brick pavement than concrete pavement.

Ficus altissima and *F. microcarpa* enjoyed significantly larger open soil area than any non-*Ficus* species at 5.859 m^2 and 3.042 m^2, respectively (Table 1b). Large-statured but non-*Ficus* species, such as *A. moluccanus*, *B. ceiba*, and *D. regia*, had intermediate mean open soil area from 1.312 to 1.689 m^2. *Lagerstroemia speciosa* had the smallest mean open soil area at 0.486 m^2.

The widest mean setback, 3.894 m, was found for *F. altissima*, significantly exceeding that of all other species (Table 1b). Large trees could be planted adjacent to narrow setback. For example, *A. moluccanus* had significantly narrower mean setback (0.376 m) than most species. Large and small trees may show statistical homogeneity in mean setback width, such as *F. microcarpa* (1.487 m) and *Xanthostemon chrysanthus* (1.353 m).

Allometric Model for TFD Prediction

For all species, DBH was a significant predictor of TFD in linear regression (Table 2a). The model with the highest R^2 value belonged to *A. alexandrae* ($R^2 = 0.804$), the only monocot in the list, whereas *Michelia* × *alba*

Table 1. Descriptive statistics of (a) dendrometric variables and (b) habitat variables of 14 tree species. Diameter at breast height, trunk flare diameter, and tree height were abbreviated as DBH, TFD, and H.

		DBH (m)			TFD (m)			H (m)			Lean (degree)		
		Mean	Median	SD	Mean	Median	SD	Mean	Median	SD	Mean	Median	SD
(a)	*Aleurites moluccanus*	0.285^{def}	0.270	0.089	0.632^{c}	0.486	0.430	10.33^{cde}	9.94	2.82	6.2^{abcd}	5.4	3.8
	Archontophoenix alexandrae	0.124^{ab}	0.116	0.033	0.254^{ab}	0.227	0.074	5.15^{a}	4.01	2.70	3.0^{a}	2.2	2.3
	Bombax ceiba	0.329^{ef}	0.314	0.111	0.653^{c}	0.548	0.336	10.06^{bcd}	9.49	3.09	4.3^{ab}	4.0	3.2
	Casuarina equisetifolia	0.254^{de}	0.261	0.108	0.636^{c}	0.602	0.338	13.45^{f}	13.13	4.94	9.0^{def}	7.8	6.2
	Cinnamomum burmannii	0.218^{cd}	0.225	0.074	0.648^{c}	0.601	0.340	8.39^{b}	8.24	2.55	10.2^{ef}	9.7	5.9
	Delonix regia	0.337^{f}	0.339	0.104	0.956^{d}	0.881	0.573	9.75^{bcd}	9.34	2.93	7.7^{cde}	6.3	5.8
	Ficus altissima	0.754^{h}	0.665	0.436	2.504^{f}	2.468	0.741	10.83^{de}	10.28	2.47	6.5^{bcd}	5.0	5.8
	Ficus microcarpa	0.467^{g}	0.434	0.182	1.797^{e}	1.718	0.523	11.94^{ef}	11.50	3.62	10.8^{ef}	8.4	8.7
	Lagerstroemia speciosa	0.129^{ab}	0.130	0.051	0.224^{a}	0.209	0.111	5.34^{a}	5.26	1.46	6.1^{abcd}	4.9	4.8
	Melaleuca cajuputi	0.205^{bcd}	0.211	0.110	0.449^{bc}	0.389	0.353	8.91^{bc}	8.73	3.19	6.3^{abcd}	5.2	4.8
	Michelia × alba	0.163^{bc}	0.170	0.080	0.223^{a}	0.217	0.097	8.31^{b}	8.22	3.48	12.1^{f}	9.5	10.8
	Photinia serratifolia	0.073^{a}	0.064	0.037	0.128^{a}	0.100	0.087	5.02^{a}	4.43	1.62	4.5^{abc}	3.3	4.5
	Spathodea campanulata	0.250^{de}	0.229	0.108	0.501^{c}	0.413	0.301	8.95^{bc}	8.58	3.25	7.6^{cde}	6.5	5.8
	Xanthostemon chrysanthus	0.068^{a}	0.062	0.024	0.124^{a}	0.111	0.049	4.81^{a}	4.75	0.82	4.0^{ab}	3.3	3.1

		Pavement width (m)			Open soil area (m^2)			Setback (m)			Pavement material		
		Mean	Median	SD	Mean	Median	SD	Mean	Median	SD	Brick	Concrete	Total
(b)	*Aleurites moluccanus*	3.467^{ab}	3.300	1.286	1.312^{cde}	1.030	1.056	0.376^{a}	0.240	0.324	50	29	79
	Archontophoenix alexandrae	5.967^{d}	3.680	3.770	0.601^{ab}	0.520	0.311	1.100^{abc}	0.885	1.014	54	4	58
	Bombax ceiba	4.007^{abc}	2.970	2.140	1.323^{cde}	1.382	0.670	1.047^{abc}	0.505	1.794	71	1	72
	Casuarina equisetifolia	9.168^{f}	9.555	2.012	1.590^{de}	1.563	0.297	2.864^{e}	2.135	1.741	118	0	118
	Cinnamomum burmannii	5.090^{cd}	5.245	2.010	1.120^{bcd}	1.081	0.552	1.998^{d}	1.293	1.627	58	10	68
	Delonix regia	5.082^{cd}	4.010	1.985	1.689^{e}	1.160	1.290	1.907^{d}	1.920	1.196	61	13	74
	Ficus altissima	7.277^{e}	7.110	1.373	5.859^{g}	5.937	2.638	3.894^{f}	4.170	1.277	58	1	59
	Ficus microcarpa	4.516^{bc}	3.535	2.571	3.042^{f}	2.781	1.522	1.487^{bcd}	0.533	2.099	74	52	126
	Lagerstroemia speciosa	5.115^{cd}	4.260	2.182	0.486^{a}	0.372	0.439	1.951^{d}	1.250	1.618	32	43	75
	Melaleuca cajuputi	4.057^{abc}	3.465	2.158	0.859^{abc}	0.665	0.622	0.845^{abc}	0.628	0.938	72	50	122
	Michelia × alba	3.530^{ab}	3.480	0.183	0.854^{abc}	0.874	0.160	2.127^{de}	2.190	0.279	0	31	31
	Photinia serratifolia	4.524^{bc}	3.640	2.019	0.834^{abc}	0.791	0.308	1.610^{cd}	1.068	1.404	41	15	56
	Spathodea campanulata	3.177^{a}	2.780	1.305	0.649^{ab}	0.464	0.409	0.709^{ab}	0.565	0.539	60	38	98
	Xanthostemon chrysanthus	4.589^{bc}	4.155	1.482	0.842^{abc}	0.814	0.326	1.353^{bcd}	0.963	1.164	52	12	64

Lower-case letters indicate results of Games-Howell comparisons using species as a fixed factor. Mean values were ranked in ascending alphabetical order. Values with the same letter indicate statistical homogeneity in their distributions.

triumphed among broadleaf trees (R^2 = 0.792). The remaining R^2 values ranged from 0.518 to 0.781, except the models of *F. altissima* and *X. chrysanthus* which featured the 2 lowest R^2 values. The largest coefficient (b_1 = 4.495 m) was found on *D. regia*, which was accompanied by the largest standard error (SE = 0.381 m).

However, DBH had lower explanatory power of TFD variation when regression models contained only trees with protruding roots and/or flares. R^2 values decreased to a range of 0.348 to 0.684 (Table 2b). For the 2 *Ficus*, limited reduction was due to the low R^2 in the original model. But among non-*Ficus* species, R^2 dropped by 0.076 to 0.297, except *D. regia*. Interestingly, R^2 remained unchanged for *D. regia*. Despite lower R^2 values, the models and the regression coefficients of DBH remained significant.

Summary of Protruding Roots and Flares

The mean length of protruding roots or flares of the 2 *Ficus* exceeded 1.0 m, being longer than other species (Table 3). For other tree species with relatively large proportions of trees with protrusions (excluding *A. alexandrae*, *L. speciosa*, *M. × alba*, *P. serratifolia*, and *X. chrysanthus*), the mean length of protruding roots and flares reached 0.484 to 0.867 m and 0.519 to 0.794 m, respectively.

Table 2. Species-specific prediction models of trunk flare diameter (TFD) using diameter at breast height (DBH) with (a) all trees under each individual species and (b) only trees with protruding roots and/or flares.

		Intercept			Regression coefficient of DBH			
		R^2	b_0	SE	b_1	SE	CI_{LOW}	CI_{UP}
(a) All trees under each individual species	*A. moluccanus*	*0.563*	−0.406	0.108	*3.645*	0.361	2.925	4.365
	A. alexandrae	*0.804*	0.005	0.017	*2.004*	0.131	1.742	2.266
	B. ceiba	*0.626*	−0.136	0.076	*2.399*	0.219	1.962	2.836
	C. equisetifolia	*0.781*	−0.066	0.037	*2.766*	0.135	2.498	3.304
	C. burmannii	*0.644*	−0.160	0.077	*3.715*	0.336	3.044	4.386
	D. regia	*0.655*	−0.559	0.134	*4.495*	0.381	3.736	5.254
	F. altissima	*0.366*	1.717	0.155	*1.044*	0.178	0.687	1.400
	F. microcarpa	*0.518*	0.829	0.089	*2.076*	0.178	1.723	2.429
	L. speciosa	*0.590*	0.009	0.022	*1.662*	0.160	1.343	1.982
	M. cajuputi	*0.667*	−0.090	0.039	*2.632*	0.169	2.298	2.966
	M. × alba	*0.792*	0.048	0.018	*1.076*	0.100	0.871	1.282
	P. serratifolia	*0.686*	−0.150	0.014	*1.944*	0.177	1.589	2.298
	S. campanulata	*0.738*	−0.100	0.039	*2.405*	0.145	2.117	2.693
	X. chrysanthus	*0.333*	0.043	0.015	*1.193*	0.209	0.775	1.611
(b) Only trees with protruding roots and/or flares	*A. moluccanus*	*0.422*	−0.078	0.246	*3.251*	0.703	1.809	4.693
	B. ceiba	*0.550*	−0.099	0.138	*2.508*	0.364	1.771	3.245
	C. equisetifolia	*0.684*	0.224	0.097	*2.222*	0.274	1.662	2.782
	C. burmannii	*0.510*	−0.085	0.133	*3.565*	0.533	2.489	4.642
	D. regia	*0.655*	−0.442	0.182	*4.464*	0.486	3.484	5.444
	F. altissima	*0.348*	1.792	0.153	*0.968*	0.174	0.619	1.317
	F. microcarpa	*0.516*	0.846	0.090	*2.053*	0.721	1.699	2.408
	M. cajuputi	*0.399*	0.031	0.141	*2.601*	0.479	1.635	3.567
	S. campanulata	*0.441*	0.028	0.185	*2.305*	0.506	1.260	3.351

The proportion of explained variance (R^2) of simple linear regression, intercept (b_0), and regression coefficient of DBH (b_1), and its standard errors (SE) were provided. The lower and upper boundary values of confidence intervals (CI_{LOW}, CI_{UP}) were computed for more conservative estimation. Significant values of R^2 and b_1 with $P < 0.05$ were italicised and underlined for easier comparison. Five species, namely *A. alexandrae*, *L. speciosa*, *M. × alba*, *P. serratifolia*, and *X. chrysanthus*, were excluded in (b) due to insufficient sample size.

Protrusion was found on 16% to 63% of samples, except for *F. altissima* with 97% and excluding those with small sample sizes (*A. alexandrae*, *L. speciosa*, *M. × alba*, *P. serratifolia*, and *X. chrysanthus*)(Table 3). The percentages of trees with protruding roots (7% to 54%) and with protruding flares (9% to 50%) were also comparable, excluding *A. alexandrae*, *F. altissima*, *L. speciosa*, *M. × alba*, *P. serratifolia*, and *X. chrysanthus*. The majority with protrusion incidents occurred in tree pits along brick pavements, reflecting the overall ratio of pavement material distribution (Table 1b).

Protrusion was uncommon among 4 species, namely *Archontophoenix alexandrae*, *L. speciosa*, *Photinia serratifolia*, and *X. chrysanthus* (Table 3). For instance, protruding roots and/or flares were found on only 5.4% of the *P. serratifolia* samples. *Michelia × alba* even had no protruding flares and roots. These 4 species, which had small or intermediate size, had yet to develop elaborate flares (Table 1a).

Prediction of Presence of Protrusion

Using logistic regression, the presence of protrusion was predicted in the 3 scenarios, namely (1) protruding roots only, (2) protruding flares only, and (3) protruding roots and/or flares as outlined in the Materials and Methods. Species-specific analyses were conducted. Nonetheless, the overall models in which all species in Table 4 were considered returned significant results. More importantly, the respective models correctly predicted the presence of protrusion in 38.3%, 53.8%, and 69.8% of cases. The rate of correct prediction was improved in species-specific models. In particular, the accuracy of predicting the presence of protruding roots was elevated to a range from 39.3% to 74.2%, excluding *C. equisetifolia* and *Ficus* spp. (Table 4a).

Sample size and distribution may affect prediction accuracy. Due to limited sample size, binary logistic regression was unable to be performed for *A. alexandrae*, *L. speciosa*, *M. × alba*, *P. serratifolia*, and

Table 3. Descriptive statistics of the length of protruding parts in 3 scenarios.

	Protruding roots						Protruding flares						Protruding roots and/or flares					
	Mean	Median	SD	Brick	Concrete	Total	Mean	Median	SD	Brick	Concrete	Total	Mean	Median	SD	Brick	Concrete	Total
A. moluccanus	0.521	0.489	0.153	5	15	20	0.736	0.723	0.289	6	8	14	0.626	0.555	0.249	10	19	29
A. alexandrae	0.144	0.144	N/A	1	0	1	0.178	0.178	0.018	2	0	2	0.167	0.165	0.024	3	0	3
B. ceiba	0.630	0.574	0.236	28	0	28	0.589	0.626	0.208	21	1	22	0.628	0.584	0.237	38	1	39
C. equisetifolia	0.586	0.578	0.148	8	0	8	0.530	0.490	0.199	16	0	16	0.564	0.536	0.192	19	0	19
C. burmannii	0.616	0.623	0.232	28	3	31	0.537	0.548	0.147	20	3	23	0.627	0.628	0.196	38	5	43
D. regia	0.867	0.708	0.495	24	3	27	0.794	0.613	0.471	29	8	37	0.870	0.689	0.500	37	8	45
F. altissima	1.334	1.227	0.522	47	1	48	1.290	1.207	0.425	50	1	51	1.419	1.306	0.472	56	1	57
F. microcarpa	1.137	0.989	1.102	42	26	68	1.060	1.042	0.387	41	19	60	1.225	1.099	0.999	48	29	77
L. speciosa	0.614	0.495	0.342	0	5	5	0.369	0.292	0.252	3	4	7	0.468	0.414	0.337	3	7	10
M. cajuputi	0.667	0.590	0.325	12	6	18	0.607	0.572	0.297	6	5	11	0.666	0.603	0.304	14	10	24
M. × alba	N/A	N/A	N/A	0	0	0	N/A	N/A	N/A	0	0	0	N/A	N/A	N/A	0	0	0
P. serratifolia	0.658	0.658	0.042	1	1	2	0.350	0.350	N/A	1	0	1	0.555	0.628	0.180	2	1	3
S. campanulata	0.484	0.406	0.173	5	4	9	0.519	0.469	0.317	5	9	14	0.527	0.456	0.297	7	10	17
X. chrysanthus	0.631	0.631	N/A	1	0	1	N/A	N/A	N/A	0	0	0	0.631	0.631	N/A	1	0	1
Total	0.896	0.725	0.739	202	64	266	0.854	0.748	0.454	200	58	258	0.899	0.737	0.680	276	91	367

The 3 scenarios were namely protruding roots, protruding flares, and protruding roots and/or flares. The statistics were computed using only trees with protruding parts. For each scenario, if more than 1 protruding part was present on a tree, the length of the longest protrusion was considered. The count of pavement materials around the tree pits with protrusion was provided. Due to the lack of protrusion or small sample size, incomputable statistics were denoted by "N/A" for *A. alexandrae*, *M. × alba*, *P. serratifolia*, and *X. chrysanthus*.

X. chrysanthus. However, for *F. altissima*, the outstanding prediction accuracy could be attributed to the fact that more than 96% of samples had protrusion (Table 4).

Of the *F. altissima* samples recorded in this research, 96.6% showed protruding roots and/or flares. Several species had more than half of the samples featuring protruding roots and/or flares, namely *B. ceiba* (54.2%), *Cinnamomum burmannii* (63.2%), *D. regia* (60.8%), and *F. microcarpa* (61.1%). Among the species in Table 4, *C. equisetifolia* had the lowest proportion, with only 16.1% of samples having protruding roots and/or flares.

DBH was a significant dendrometric predictor in many cases. Overviewing the 3 scenarios, a centimetre increment in DBH resulted in 1.049 to 1.262 times greater odds ratio of protrusion (Table 4). Trunk lean increased the likelihood of protruding roots (Table 4a). For habitat predictors, open soil area had large positive coefficients due to the measurement unit (m^2). Also, if trees were growing in tree pits on concrete pavement, the odds ratio of protrusion would be higher than those on brick pavement. *Aleurites moluccanus* growing on concrete pavement saw an increase of 15.625 times, which was the reciprocal of the change to odd ratio by brick pavement (0.064), in the model for protruding roots only (Table 4a). Also, *Spathodea campanulata*, which was planted in tree pits on concrete pavement, had 11.236 and 9.009 times greater likelihood of protruding roots and flares, respectively (Table 4a, 4b). These values were obtained by computing the reciprocal of the effects on odds ratio in Table 4. When protruding roots and/or flares were considered together, *S. campanulata* along concrete pavement had 17.857 times greater the likelihood of protrusion (Table 4c). Being less permeable than brick pavement, concrete pavement might force the root system of trees to expand to harvest the required moisture and nutrients. Yet the likelihood of protruding flares of *F. microcarpa* along brick pavement was 7.659 times those of trees along concrete pavement.

Prediction of Magnitude of Protrusion

General models without the distinction of tree species were significant, explaining 20.7%, 57.7%, and 31.1% variation in the length of protruding roots, protruding flares, and protruding roots and/or flares, respectively (Table 5). Most of the species-specific models, if significant, explained more variance in the length of protruding parts than the general models. The significance of results might depend on prediction scenario. For *B. ceiba*, model significance only

Table 4. Binary logistic regression results predicting the occurrence of (a) protruding roots, (b) protruding flares, and (c) protruding roots and/or flares. Diameter at breast height and tree height were abbreviated as DBH and H.

		Model statistics				Effects on odds ratio							
		X^2	R^2	Yes%	No%	Intercept	DBH	H	Lean	Pavement width	Open soil area	Setback	Pavement material (brick)
(a) Protruding roots only	*A. moluccanus*	*22.43*	0.365	55.0	89.8	0.336	1.081	1.056	0.904	1.101	0.319	2.083	*0.064*
	B. ceiba	*15.58*	0.264	39.3	86.4	0	1.006	1.022	0.979	0.374	3.749	7.102	∞
	C. equisetifolia	*15.53*	0.247	15.4	99.0	∞	*1.146*	0.973	0.917	0.923	0	1.242	N/A
	C. burmannii	*33.44*	0.519	74.2	83.8	0	0.963	*1.471*	*1.277*	1.435	*10.700*	0.850	0.534
	D. regia	*14.98*	0.251	40.7	87.2	0.105	1.048	0.828	1.105	0.747	1.707	1.046	7.128
	F. altissima	11.88	0.295	93.8	27.3	∞	1.011	1.163	1.169	*0.423*	0.777	2.007	0
	F. microcarpa	5.01	0.061	100.0	0	3.401	0.998	0.936	1.014	1.144	1.162	1.058	0.724
	M. cajuputi	*26.83*	0.287	39.4	94.4	0.011	1.086	1.049	0.984	1.095	1.486	1.352	1.840
	S. campanulata	*42.85*	0.616	73.3	96.4	0	*1.241*	1.006	0.924	1.424	2.959	0.997	*0.089*
	All trees	*273.84*	0.314	38.3	94.2	0.064	*1.049*	1.014	*1.028*	0.934	*1.269*	1.110	0.958
(b) Protruding flares only	*A. moluccanus*	*38.63*	0.637	64.3	96.9	0	1.158	0.948	1.112	0.278	*32.930*	165.600	5.516
	B. ceiba	*16.53*	0.290	31.8	88.0	∞	1.086	0.921	0.896	0.598	2.170	1.456	0
	C. equisetifolia	*35.55*	0.409	41.7	94.7	0	*1.262*	0.927	0.960	1.001	39.110	0.966	N/A
	C. burmannii	12.88	0.239	52.2	86.7	0.196	*1.130*	1.018	0.942	0.766	0.357	1.475	1.471
	D. regia	*17.71*	0.284	64.9	64.9	0.047	1.078	1.067	0.990	0.721	1.345	1.174	2.901
	F. altissima	10.68	0.302	100.0	37.5	∞	1.020	1.464	0.950	1.326	0.949	0.708	0
	F. microcarpa	*27.65*	0.312	95.0	28.0	0.032	*1.051*	1.083	0.980	1.031	1.524	0.926	*7.659*
	M. cajuputi	*25.11*	0.296	12.5	95.9	0.007	*1.137*	0.988	1.018	1.101	0.713	0.952	2.061
	S. campanulata	*39.96*	0.518	52.4	94.8	0.002	1.075	1.177	1.080	1.001	12.800	0.901	*0.111*
	All trees	*468.80*	0.493	53.8	94.0	0.015	*1.102*	1.000	1.008	0.972	*1.287*	1.056	1.222
(c) Protruding roots and/or flares	*A. molp6uccanus*	*36.93*	0.511	69.0	90.0	0.013	1.120	1.019	0.999	0.858	1.646	12.130	0.227
	B. ceiba	*24.74*	0.389	66.7	72.7	∞	1.008	1.119	0.899	*0.188*	*7.540*	23.080	0
	C. equisetifolia	*36.11*	0.385	41.9	95.4	0	*1.224*	0.938	0.935	0.910	44.020	1.074	N/A
	C. burmannii	*24.53*	0.414	81.4	64.0	0.006	1.053	1.387	1.071	0.602	6.987	1.891	1.876
	D. regia	12.73	0.214	77.8	31.0	0.291	1.030	0.987	1.009	0.642	1.954	1.311	5.918
	F. altissima	*17.47*	1.000	100.0	100.0	∞	1.829	∞	0.565	0	0.008	0	∞
	F. microcarpa	*15.37*	0.570	100.0	33.3	∞	0.988	0.796	0.742	0	51.100	∞	∞
	M. cajuputi	*42.88*	0.406	59.1	83.3	0.007	*1.111*	1.107	0.981	1.033	1.488	1.283	2.457
	S. campanulata	*55.91*	0.634	69.2	93.1	0	1.088	*1.346*	1.072	1.118	20.480	1.036	*0.056*
	All trees	*540.1*	0.523	69.8	87.9	0.034	*1.114*	0.980	1.003	0.916	*1.758*	1.132	0.956

The rates of correct prediction of the presence (Yes%) and absence (No%) of protrusion were provided. Species-specific effects of DBH in centimetres, H, lean angle, pavement width, open soil area, setback, and pavement material on the odds ratio of the occurrence of the 3 scenarios were reported. "N/A" indicated a lack of variation. Significant model statistics and predictors with $P < 0.05$ were italicised and underlined. For comparison, the pseudo-R^2 values were supplied. *A. alexandrae*, *L. speciosa*, *M.* × *alba*, *P. serratifolia*, and *X. chrysanthus* were excluded due to small sample size.

occurred in the prediction of length of protruding roots (Table 5a). However, for *D. regia*, the models were significant regardless of prediction scenario.

Open soil area, which was a habitat factor, explained the length of protruding parts significantly in many models (Table 5). In the general model, uniformity was observed in the coefficient value of open soil area. A square-metre increase in open soil area prolonged the protruding part by 0.154 to 0.172 m. Some species, such as *S. campanulata*, showed even greater response, ranging from 0.416 to 0.446 m.

Among dendrometric factors, lean angle was a significant factor in several models. Despite its seemingly small regression coefficients from 0.007 to 0.041 times higher likelihood for an increase in lean by a degree, the practical effects could be interpreted with the possible extent of leaning. For example, *B. ceiba*, which featured the largest regression coefficient (0.041), would bear 0.178-m protruding roots given the mean lean angle at 4.34° (Tables 1a and 5a).

Table 5. Multiple regression results for predicting the length of (a) protruding roots, (b) protruding flares, and (c) protruding roots and/or flares. Diameter at breast height and tree height were abbreviated as DBH and H.

			R^2	Intercept	DBH	H	Lean angle	Pavement width	Open soil area	Setback	Pavement material
(a)	Protruding roots only	*A. moluccanus*	0.203	0.711	−0.038	−0.002	0.004	−0.022	0.091	−0.454	−0.003
		B. ceiba	*0.285*	−0.039	−0.782	0.060	*0.041*	0.043	0.018	−0.050	0
		C. equisetifolia	0.192	0.451	−0.882	0.026	0.006	0.013	−0.048	0	N/A
		C. burmannii	*0.668*	0.519	0.684	−0.017	0.002	*−0.095*	*0.292*	*0.102*	−0.018
		D. regia	*0.639*	−0.012	0.422	−0.018	−0.020	−0.043	*0.168*	0.086	*0.713*
		F. altissima	*0.338*	1.069	−0.084	0.017	−0.004	−0.166	*0.099*	*0.267*	−0.223
		F. microcarpa	0.017	−0.032	0.730	0	−0.005	0.032	0.119	−0.053	0.321
		M. cajuputi	*0.624*	0.132	0.373	0.008	0.007	0.010	*0.246*	*0.069*	−0.076
		S. campanulata	0.502	0.849	−0.750	−0.010	−0.003	−0.020	*0.428*	−0.054	−0.206
		All trees	*0.207*	0.219	0.024	0.007	0	−0.009	*0.165*	0.006	0.158
(b)	Protruding flares only	*A. moluccanus*	0.127	0.239	−1.425	−0.009	−0.004	0.306	0.157	−0.623	0.006
		B. ceiba	0.124	0.627	−0.602	0.002	0.002	−0.066	0.276	0.116	−0.116
		C. equisetifolia	*0.449*	0.405	0.516	*−0.029*	*0.015*	−0.024	*0.195*	*0.076*	N/A
		C. burmannii	0.164	0.386	0.675	0.002	0.004	0.043	−0.224	*−0.081*	0.111
		D. regia	*0.590*	0.347	0.026	−0.016	0.003	−0.046	*0.234*	0.034	0.205
		F. altissima	*0.294*	2.290	−0.005	0.001	−0.009	−0.115	*0.078*	0.101	*−0.952*
		F. microcarpa	*0.479*	0.320	*0.511*	−0.008	0.004	0.007	*0.142*	−0.027	0.080
		M. cajuputi	*0.759*	0.014	−1.193	−0.013	0.016	−0.007	*0.492*	*0.095*	*0.292*
		S. campanulata	*0.756*	−0.595	−0.835	0.030	*0.019*	0.037	*0.416*	−0.020	0.222
		All trees	*0.577*	0.306	0.051	0	*0.007*	−0.014	*0.154*	0.001	*0.092*
(c)	Protruding roots and/or flares	*A. moluccanus*	*0.398*	0.660	−0.745	0.006	0.004	0.016	*0.169*	−0.427	−0.013
		B. ceiba	0.167	0.428	−0.010	0.009	*0.028*	−0.062	0.158	0.063	−0.053
		C. equisetifolia	0.196	0.134	0.312	−0.008	*0.013*	−0.002	0.148	0.050	N/A
		C. burmannii	*0.475*	0.237	0.536	0.001	0.003	−0.007	*0.207*	−0.016	0.024
		D. regia	*0.633*	0.397	1.072	−0.053	0.007	−0.066	*0.220*	0.068	0.286
		F. altissima	*0.359*	1.509	−0.051	0.008	−0.010	*−0.158*	*0.103*	*0.208*	−0.311
		F. microcarpa	*0.098*	−0.207	1.110	−0.001	0.001	0.035	0.130	−0.064	0.327
		M. cajuputi	*0.662*	0.126	0.432	−0.002	0.009	0.010	*0.266*	*0.071*	−0.019
		S. campanulata	*0.630*	−0.319	−0.364	0.013	*0.015*	0.012	*0.446*	−0.015	0.127
		All trees	*0.311*	0.185	0.164	0.003	0.008	−0.014	*0.172*	0.002	*0.159*

In each scenario, if more than 1 protrusion was detected on a tree, only the longest protruding parts were considered. Species-specific regression coefficients of the predictors, namely DBH, H, lean angle, pavement width, open soil area, setback, and pavement material, were presented. If significant, the adjusted R^2 and regression coefficient values were italicised and underlined. "N/A" indicated a lack of variation. *A. alexandrae*, *L. speciosa*, *M. × alba*, *P. serratifolia*, and *X. chrysanthus* were excluded due to small sample size.

DISCUSSION

Measurement Method of Trunk Flare

TFD prediction models in Table 2 were corroborated by previous studies in the sense that DBH was the critical predictor of TFD (North et al. 2015; Hilbert et al. 2020). However, in terms of R^2 values from DBH-TFD models, the past researchers reported much-higher values ($R^2 > 0.80$) than those in the present research ($R^2 \leq 0.792$), except for *A. alexandrae*. However, most of the regression coefficients of DBH in this study, which were up to 4.495 m, exceeded the values documented in the previous studies (1.3 to 1.9 m). In short, DBH showed a stronger effect in TFD prediction models with lower R^2 than in past research.

The discrepancy could be caused by the difference in measurement methods. In previous research, TFD was marked at the points of transition from trunk to root at ground level. However, in the current research, protruding roots and/or flares were observed to encroach on pavement surface. As the outermost points of protruding roots and/or flares, if present, were used in the measurement of TFD (Figure 2), larger TFD values with greater variability could thus

be expected. Consequently, the measurement protocol of this research would raise the regression coefficient values of DBH. The higher variability rendered more TFD variation unexplainable.

The differences in the explained variances between the current and the past studies highlighted the importance of a simple, consistent, and reliable variable for the quantification of trunk flares. Existing sensing technologies, such as unmanned aerial vehicles and LiDAR, help measure DBH and height in forest sites (Birdal et al. 2017; Panagiotidis et al. 2017; Torresan et al. 2017; Kwong and Fung 2020). But technologies are yet to be developed for trunk flare measurement. From the perspective of tree surveyors, work efficiency could be enhanced by standardising the measurement protocol by specifying that the outermost points of trunk flares should be measured. Although such methods introduced more unexplained variation, DBH-TFD models were still significant. Also, the conflict between tree roots and/or flares and pavement surface could be characterised. Therefore, the methods of trunk flare measurement could be updated to the approach as in this research.

Effects of Sample Selection on TFD Prediction

The performance of DBH-TFD prediction models dropped discernibly if the examined sample was solely composed of trees with protruding roots and/or flares (Table 2b). In fact, TFD values were directly and positively linked to the length of protruding parts which could have rather high variance (Table 3). Such variance would by default influence the variation in TFD, subsequently inflating errors but diminishing the explanatory power of DBH. Protruding parts created variable and disproportionate increase in TFD in relation to DBH. As a result, the model significance and the regression coefficients of DBH decreased.

Landscape architects who need to estimate planting space requirements may be troubled by the less-reliable models containing only trees with protruding roots and/or flares. Preventing pavement damage by large-stature species such as *A. moluccanus*, *C. equisetifolia*, and *Melaleuca cajuputi* may become difficult. Worse still, singling out samples with protrusion resulted in divergent directions of change in regression coefficients. Fearing underestimated TFD, landscape architects may refrain from using the reduced regression coefficients caused by the change in sample selection (Table 2b). Without a sufficiently large open soil area, the outward stress caused by the trunk flares of large trees may be detrimental to the pavement.

Despite the uncertainties, the confidence intervals of regression coefficient of DBH could be utilised in various scenarios (Table 2). Along wide pavements, the upper boundary value (CI_{UP}) of the regression coefficient of DBH could be used to generate larger TFD estimates, justifying the provision of extra buffer space. For narrow pavement, TFD could be predicted using the lower boundary value (CI_{LOW}) at the acceptable risk of pavement damage. Unless the open soil area requirement was met as advised by TFD estimates, landscape planners should switch to another suitable species with smaller TFD. This suggestion echoes the strategy of planting small-stature trees in cramped spaces (Blunt 2008). The confidence intervals could only be computed when sample size and standard error are available. Therefore, for a more-detailed record-keeping purpose, these critical values should be reported in future studies on DBH-TFD allometry.

Recommendations for Landscape Planning

In all 3 scenarios, diameter growth significantly increased the likelihood of protrusion (Table 4). Such findings agree with Hilbert et al. (2020). Nonetheless, by using species-specific prediction and comprehensive model outputs, the effects of habitat factors on the occurrence of protrusion were captured. There was a difference in the nature of significant predictors of the presence and magnitude of protrusion. Dendrometric and habitat factors explained the majority of variations in the presence and magnitude of protruding parts, respectively (Tables 4 and 5). Regardless, the apparent contradiction was resolved by reading the correlations among predictors. The highest correlations, which were also significant, were found between DBH and soil area ($0.376 < r < 0.755$). In other words, thick-stemmed trees with higher DBH correlated to larger soil area. Such observations are sensible, as a larger tree pit would be necessary to accommodate larger trees whose larger DBH are in turn linked to higher likelihood of protrusion.

More sustainable landscape planning could be enabled with the use of such models. With known

DBH values, the odds ratio of protrusion could be computed and compared among possible tree species to be selected (Table 4). An acceptable odds ratio would imply a species' suitability for roadside greening. The required open soil area could then be calculated with species-specific regression equations (Table 5). A database archiving the key dimensions of a mature specimen of the selected tree species would be necessary. The known values related to tree species as well as planned pavement configurations could be substituted into the equation. Normally, protruding roots and/or flares would stick out from the tree stem located in the tree pit centre. Therefore, in order to avoid pavement damage and tree-health decline, the halved length and width of the open soil area must exceed the predicted magnitude of protrusion. If exceeded, an expansion in the open soil area would be required. For existing trees showing signs of potential protrusion, tree-pit enlargement could be justified by regression outputs generated in the manner of this study.

In some studies, substrate amendments such as a gravel base layer or structural cell and soil texture modifications were shown to buffer root diameter growth and direct roots downward (Smiley 2008; Rahardjo et al. 2016; Giuliani et al. 2017; Ow and Ghosh 2017; Johnson et al. 2019; Lucke and Beecham 2019). In the case of tree pits on pavement, the possibility of using such measures may be restricted. The required load-bearing capacity may be offered by intentional compaction of backfilled, native, fine-soil particles without additional structures. Eventually, the chief strategy must be to reserve sufficient open soil area for healthy tree growth.

The enormous amount of information in Tables 4 and 5 may be overwhelming. The complexity posed a huge contrast to the simple allometric equations presented in past studies (e.g., Hilbert et al. 2020). In fact, a reduced set of significant predictors could be conveniently distilled using hierarchical and stepwise regression. However, in this non-interventional tree survey, experimental control was severely limited. Total control of planting environment was impractical. Hence, with the ability to exercise statistical control, simultaneous regression was preferred (Keith 2019). Nevertheless, future studies could be conducted in the format of controlled experiments.

Limitations and Future Studies

Pavement damages may occur well before protruding roots and/or flares touch the edge of paving materials. In fact, during the tree survey, spalling and cracks were observed even when flares and roots were yet to be reckoned as protruding. Techniques such as ground-penetrating radar, of course, could facilitate the detection of root architecture which is invisible at the surface. Root position of urban trees, mostly up to 0.6 m deep, would be detectable within the reach of ground-penetrating radar in urban applications (Jim 2003; Grabosky and Bassuk 2016; Altdorff et al. 2019). Although technically possible, the time and financial costs might render these technologies ineffective, if not impractical, for a district-wide sampling as in the present research. The propensity of protrusion to create damage merits another lengthy examination. When further analyses are published, the understanding of protruding roots and/or flares as an indicator of pavement damages can be improved.

Physiological compromises related to the tree roots were not examined in this study. It is acknowledged that deep burying, girdling roots, and root pruning may hinder initial tree establishment, taper development, and reduce the long-term survival of urban trees (Arnold et al. 2005; Arnold et al. 2007; Blunt 2008; Day and Harris 2008; Day et al. 2009; Gilman and Grabosky 2011; Benson et al. 2019a, 2019b). While root-related defects had been noted during the tree survey, the present research was purposed to analyse the dendrometric and habitat measurements with attention to the protruding parts of the trees. A future research direction would be to expand the allometric analysis in this study to tree defects and disorders, not just in the root-soil system, but also on other parts of trees.

CONCLUSION

In this study, protruding roots and flares, in tandem with other dendrometric and habitat factors, were measured. Emphasis was placed on trees growing in tree pits along pavements built with bricks or concrete. Various statistical comparisons and regression models were carried out to quantify the relationships between pavements and trees. Among 14 species, 1,100 trees showed complex patterns and divergence in the distributions of key dimensions and habitat conditions. Based on linear regression, allometric relationships between DBH and TFD were established. DBH was a significant predictor of TFD. But DBH-TFD relationships were weakened if only trees with protruding roots and/or flares were included in the prediction models. Still, with the purpose of avoiding pavement damage, more conservative TFD estimates

could be obtained with the assistance of the confidence intervals of regression coefficients. Most logistic and multiple regression models for the occurrence and magnitude of protruding roots and/or flares were significant. In many cases, the odds ratio of protruding roots and/or flares increased with DBH. On the other hand, the length of protruding roots and/or flares increased with open soil area. Using the regression coefficients and the intercepts summarised in the tables, it is possible to estimate the likelihood and possible extent of protrusion. In an urban planning context where pavements are dotted with trees, the selection and care of trees can be informed using the quantitative approach demonstrated in this study. In future research, the potential linkages between tree physiological compromises and protruding roots and/or flares could be explored with the help of the latest technologies for monitoring the underground root system.

LITERATURE CITED

Altdorff D, Botschek J, Honds M, van der Kruk J, Vereecken H. 2019. In situ detection of tree root systems under heterogeneous anthropogenic soil conditions using ground penetrating radar. *Journal of Infrastructure Systems*. 25(3):05019008. https://doi.org/10.1061/(ASCE)IS.1943-555X.0000501

Arnold MA, McDonald GV, Bryan DL. 2005. Planting depth and mulch thickness affect establishment of green ash (*Fraxinus pennsylvanica*) and bougainvillea goldenraintree (*Koelreuteria bipinnata*). *Journal of Arboriculture*. 31(4):163-170. https://doi.org/10.48044/jauf.2005.021

Arnold MA, McDonald GV, Bryan DL, Denny GC, Watson WT, Lombardini L. 2007. Below-grade planting adversely affects survival and growth of tree species from five different families. *Arboriculture & Urban Forestry*. 33(1):64-69. https://doi.org/10.48044/jauf.2007.008

Barker PA, Peper PJ. 1995. Strategies to prevent damage to sidewalks by tree roots. *Arboricultural Journal*. 19(3):295-309. https://doi.org/10.1080/03071375.1995.9747072

Bartens J, Day SD, Harris JR, Wynn TM, Dove JE. 2009. Transpiration and root development of urban trees in structural soil stormwater reservoirs. *Environ Manage*. 44(4):646-657. https://doi.org/10.1007/s00267-009-9366-9

Benson AR, Koeser AK, Morgenroth J. 2019a. Responses of mature roadside trees to root severance treatments. *Urban Forestry & Urban Greening*. 46:126448. https://doi.org/10.1016/j.ufug.2019.126448

Benson AR, Morgenroth J, Koeser AK. 2019b. The effects of root pruning on growth and physiology of two *Acer* species in New Zealand. *Urban Forestry & Urban Greening*. 38:64-73. https://doi.org/10.1016/j.ufug.2018.11.006

Birdal AC, Avdan U, Türk T. 2017. Estimating tree heights with images from an unmanned aerial vehicle. *Geomatics, Natural Hazards and Risk*. 8(2):1144-1156. https://doi.org/10.1080/19475705.2017.1300608

Blunt SM. 2008. Trees and pavements—Are they compatible? *Arboricultural Journal*. 31(2):73-80. https://doi.org/10.1080/03071375.2008.9747522

Census and Statistics Department. 2018. 2016 Population By-census. Wan Chai (Hong Kong): The Government of the Hong Kong Special Administrative Region. [Accessed 2021 July 5]. https://www.censtatd.gov.hk/en/scode459.html

Chen Y, Wang X, Jiang B, Wen Z, Yang N, Li L. 2017. Tree survival and growth are impacted by increased surface temperature on paved land. *Landscape and Urban Planning*. 162:68-79. https://doi.org/10.1016/j.landurbplan.2017.02.001

Cheung PK, Jim CY. 2018. Comparing the cooling effects of a tree and a concrete shelter using PET and UTCI. *Building and Environment*. 130:49-61. https://doi.org/10.1016/j.buildenv.2017.12.013

D'Amato NE, Sydnor TD, Knee M, Hunt R, Bishop B. 2002. Which comes first, the root or the crack? *Journal of Arboriculture*. 28(6):277-282. https://doi.org/10.48044/jauf.2002.041

Day SD, Harris JR. 2008. Growth, survival, and root system morphology of deeply planted *Corylus colurna* 7 years after transplanting and the effects of root collar excavation. *Urban Forestry & Urban Greening*. 7(2):119-128. https://doi.org/10.1016/j.ufug.2007.12.004

Day SD, Watson G, Wiseman PE, Harris JR. 2009. Causes and consequences of deep structural roots in urban trees: From nursery production to landscape establishment. *Arboriculture & Urban Forestry*. 35(4):182-191. https://doi.org/10.48044/jauf.2009.031

Ebrahimian A, Gulliver JS, Wilson BN. 2018. Estimating effective impervious area in urban watersheds using land cover, soil character and asymptotic curve number. *Hydrological Sciences Journal*. 63(4):513-526. https://doi.org/10.1080/02626667.2018.1440562

Gilman EF, Grabosky J. 2011. *Quercus virginiana* root attributes and lateral stability after planting at different depths. *Urban Forestry & Urban Greening*. 10(1):3-9. https://doi.org/10.1016/j.ufug.2010.09.005

Giuliani F, Autelitano F, Degiovanni E, Montepara A. 2017. DEM modelling analysis of tree root growth in street pavements. *International Journal of Pavement Engineering*. 18(1):1-10. https://doi.org/10.1080/10298436.2015.1019495

Grabosky J, Bassuk N. 2016. Seventeen years' growth of street trees in structural soil compared with a tree lawn in New York City. *Urban Forestry & Urban Greening*. 16:103-109. https://doi.org/10.1016/j.ufug.2016.02.002

Grabosky J, Gucunski N. 2019. Modelling the influence of root position and growth on pavement tensile crack failure when occurring under three thicknesses of asphaltic concrete. *Urban Forestry & Urban Greening*. 41:238-247. https://doi.org/10.1016/j.ufug.2019.04.006

Grabosky J, Haffner E, Bassuk N. 2009. Plant available moisture in stone-soil media for use under pavement while allowing urban tree root growth. *Arboriculture & Urban Forestry*. 35(5):271-278. https://doi.org/10.48044/jauf.2009.041

Greening, Landscape & Tree Management Section Development Bureau. 2021. Planting Record. Wan Chai (Hong Kong): The Government of the Hong Kong Special Administrative Region. [Updated 2021 December 10; Accessed 2021 July 5]. https://

www.greening.gov.hk/en/greening-landscape/planting-record/index.html

Hilbert DR, North EA, Hauer RJ, Koeser AK, McLean DC, Northrop RJ, Andreu M, Parbs S. 2020. Predicting trunk flare diameter to prevent tree damage to infrastructure. *Urban Forestry & Urban Greening*. 49:126645. https://doi.org/10.1016/j.ufug.2020.126645

Islam MN, Rahman KS, Bahar MM, Habib MA, Ando K, Hattori N. 2012. Pollution attenuation by roadside greenbelt in and around urban areas. *Urban Forestry & Urban Greening*. 11(4):460-464. https://doi.org/10.1016/j.ufug.2012.06.004

Jim CY. 2003. Protection of urban trees from trenching damage in compact city environments. *Cities*. 20(2):87-94. https://doi.org/10.1016/S0264-2751(02)00096-3

Johnson T, Moore G, Cameron D, Brien C. 2019. An investigation of tree growth in permeable paving. *Urban Forestry & Urban Greening*. 43:126374. https://doi.org/10.1016/j.ufug.2019.126374

Keith TZ. 2019. *Multiple regression and beyond: An introduction to multiple regression and structural equation modeling*. 3rd Ed. New York (NY, USA): Routledge. https://doi.org/10.4324/9781315162348

Krainyukov A, Lyaksa I. 2016. Detection of tree roots in an urban area with the use of ground penetrating radar. *Transport and Telecommunication Journal*. 17(4):362-370. https://doi.org/10.1515/ttj-2016-0032

Kwong IHY, Fung T. 2020. Tree height mapping and crown delineation using LiDAR, large format aerial photographs, and unmanned aerial vehicle photogrammetry in subtropical urban forest. *International Journal of Remote Sensing*. 41(14):5228-5256. https://doi.org/10.1080/01431161.2020.1731002

Lee LS, Cheung PK, Fung CK, Jim CY. 2020. Improving street walkability: Biometeorological assessment of artificial-partial shade structures in summer sunny conditions. *International Journal of Biometeorology*. 64(4):547-560. https://doi.org/10.1007/s00484-019-01840-9

Lee LSH, Zhang H, Jim CY. 2021. Serviceable tree volume: An alternative tool to assess ecosystem services provided by ornamental trees in urban forests. *Urban Forestry & Urban Greening*. 59:127003. https://doi.org/10.1016/j.ufug.2021.127003

Li J, Guo L. 2017. Field investigation and numerical analysis of residential building damaged by expansive soil movement caused by tree root drying. *Journal of Performance of Constructed Facilities*. 31(1):D4016003. https://doi.org/10.1061/(ASCE)CF.1943-5509.0000908

Loprencipe G, Pantuso A. 2017. A specified procedure for distress identification and assessment for urban road surfaces based on PCI. *Coatings*. 7(5):65. https://doi.org/10.3390/coatings7050065

Lucke T, Beecham S. 2019. An infiltration approach to reducing pavement damage by street trees. *Science of the Total Environment*. 671:94-100. https://doi.org/10.1016/j.scitotenv.2019.03.357

Mann PS. 2007. *Introductory statistics*. 6th Ed. Hoboken (NJ, USA): John Wiley & Sons.

Marziliano PA, Lafortezza R, Colangelo G, Davies C, Sanesi G. 2013. Structural diversity and height growth models in urban forest plantations: A case-study in northern Italy. *Urban Forestry & Urban Greening*. 12(2):246-254. https://doi.org/10.1016/j.ufug.2013.01.006

Morgenroth J, Buchan GD. 2009. Soil moisture and aeration beneath pervious and impervious pavements. *Arboriculture and Urban Forestry*. 35(3):135-141. https://doi.org/10.48044/jauf.2009.024

Mullaney J, Lucke T, Trueman SJ. 2015. A review of benefits and challenges in growing street trees in paved urban environments. *Landscape and Urban Planning*. 134:157-166. https://doi.org/10.1016/j.landurbplan.2014.10.013

North EA, Johnson GR, Burk TE. 2015. Trunk flare diameter predictions as an infrastructure planning tool to reduce tree and sidewalk conflicts. *Urban Forestry & Urban Greening*. 14(1):65-71. https://doi.org/10.1016/j.ufug.2014.11.009

Oldfield EE, Felson AJ, Auyeung DSN, Crowther TW, Sonti NF, Harada Y, Maynard DS, Sokol NW, Ashton MS, Warren RJ II, Hallett RA, Bradford MA. 2015. Growing the urban forest: Tree performance in response to biotic and abiotic land management. *Restoration Ecology*. 23(5):707-718. https://doi.org/10.1111/rec.12230

O'Sullivan OS, Holt AR, Warren PH, Evans KL. 2017. Optimising UK urban road verge contributions to biodiversity and ecosystem services with cost-effective management. *Journal of Environmental Management*. 191:162-171. https://doi.org/10.1016/j.jenvman.2016.12.062

Ow LF, Ghosh S. 2017. Urban tree growth and their dependency on infiltration rates in structural soil and structural cells. *Urban Forestry & Urban Greening*. 26:41-47. https://doi.org/10.1016/j.ufug.2017.06.005

Ozer S, Irmak MA, Yilmaz H. 2008. Determination of roadside noise reduction effectiveness of *Pinus sylvestris L.* and *Populus nigra L.* in Erzurum, Turkey. *Environmental Monitoring and Assessment*. 144(1-3):191-197. https://doi.org/10.1007/s10661-007-9978-6

Panagiotidis D, Abdollahnejad A, Surový P, Chiteculo V. 2017. Determining tree height and crown diameter from high-resolution UAV imagery. *International Journal of Remote Sensing*. 38(8-10):2392-2410. https://doi.org/10.1080/01431161.2016.1264028

Planning Department. 2020. Land Utilization in Hong Kong 2020. Wan Chai (Hong Kong): The Government of the Hong Kong Special Administrative Region. [Accessed 2021 July 5]. https://www.pland.gov.hk/pland_en/info_serv/statistic/landu.html

Rahardjo H, Gofar N, Amalia N, Leong EC, Ow LF. 2016. Structural cell contribution to resistance of trees to uprooting. *Trees*. 30(5):1843-1853. https://doi.org/10.1007/s00468-016-1417-2

Rotherham ID. 2010. Thoughts on the politics and economics of urban street trees. *Arboricultural Journal*. 33(2):69-75. https://doi.org/10.1080/03071375.2010.9747596

Semenzato P, Cattaneo D, Dainese M. 2011. Growth prediction for five tree species in an Italian urban forest. *Urban Forestry & Urban Greening*. 10(3):169-176. https://doi.org/10.1016/j.ufug.2011.05.001

Smiley ET. 2008. Comparison of methods to reduce sidewalk damage from tree roots. *Arboriculture & Urban Forestry*. 34(3):179-183. https://doi.org/10.48044/jauf.2008.024

Stovin VR, Jorgensen A, Clayden A. 2008. Street trees and stormwater management. *Arboricultural Journal*. 30(4):297-310. https://doi.org/10.1080/03071375.2008.9747509

Timm A, Kluge B, Wessolek G. 2018. Hydrological balance of paved surfaces in moist mid-latitude climate–A review. *Landscape and Urban Planning*. 175:80-91. https://doi.org/10.1016/j.landurbplan.2018.03.014

Torresan C, Berton A, Carotenuto F, Di Gennaro SF, Gioli B, Matese A, Miglietta F, Vagnoli C, Zaldei A, Wallace L. 2017. Forestry applications of UAVs in Europe: A review. *International Journal of Remote Sensing*. 38(8-10):2427-2447. https://doi.org/10.1080/01431161.2016.1252477

Watson GW, Hewitt AM, Custic M, Lo M. 2014. The management of tree root systems in urban and suburban settings II: A review of strategies to mitigate human impacts. *Arboriculture & Urban Forestry*. 40(5):249-271. https://doi.org/10.48044/jauf.2014.025

Zheng B, Myint SW, Fan C. 2014. Spatial configuration of anthropogenic land cover impacts on urban warming. *Landscape and Urban Planning*. 130:104-111. https://doi.org/10.1016/j.landurbplan.2014.07.001.

ACKNOWLEDGMENTS

This research was supported by a Seed Grant of Technological and Higher Education of Hong Kong (1920114). I would like to thank Phoebe Luk, Cassandra Lo, Gym Li, and Issac Luk for their assistance in the field work.

Louis S.H. Lee (corresponding author)
Department of Environment
Faculty of Design and Environment
Technological and Higher Education Institute of Hong Kong
133 Shing Tai Road
Chai Wan, Hong Kong, China
+852-3890-8287
louislee@thei.edu.hk

Conflicts of Interest:
The author reported no conflicts of interest.

Résumé. Contexte: Les fosses d'arbres dans les zones pavées constituent des infrastructures vertes urbaines. Mais les racines et l'empattement du tronc des arbres, particulièrement des plus gros, peuvent entrer en conflit avec le recouvrement pavé, entraînant un déclin de la condition des arbres et la nécessité de coûts de réparation. Cette étude visait à (1) établir des relations allométriques entre le diamètre à hauteur de poitrine (DHP) et le diamètre d'empattement du tronc (DET) d'espèces d'arbres urbaines usuelles et (2) identifier les facteurs affectant la présence et l'ampleur des racines saillantes et des empattements protubérants. Méthodes: Les termes "racines saillantes" et "empattements protubérants" ont été strictement définis comme des racines et des empattements atteignant ou dépassant la limite entre la pleine terre et le niveau du pavage adjacent. L'étude a porté sur 1 100 arbres répartis en 14 espèces plantées dans des fosses d'arbres à Chai Wan, Hong Kong. Résultats: Le DHP était un indice significatif du DET mais il était moins significatif lorsque les arbres avec des racines ou des empattements saillants étaient considérés séparément. Dans la plupart des modèles logistiques, le DHP était significativement et positivement lié avec la probabilité d'occurrence de racines et d'empattements saillants. Globalement, l'augmentation du DHP d'un centimètre entraînait une probabilité de 1,049 à 1,114 fois plus élevée de racines saillantes et d'empattements protubérants. La régression multiple suggère que, pour chaque mètre carré d'augmentation de la superficie de pleine terre dans les fosses d'arbres, la longueur maximale des racines saillantes et des empattements augmentait de 0,154 à 0,172 m. Cette relation pourrait être attribuée à l'association sous-jacente entre le DHP et la superficie de pleine terre de la fosse. Les résultats de la régression particulière à chaque espèce ont été présentés sous forme de tableau afin de permettre une anticipation plus précise des racines saillantes et des empattements. Conclusion: Pour les urbanistes et les ingénieurs des chaussées, l'approche recommandée dans cette étude pourrait être adoptée afin d'optimiser le verdissement urbain et la conception des chaussées.

Zusammenfassung. Hintergrund: Baumgruben sind städtische grüne Infrastrukturen in gepflasterten Bereichen. Allerdings können Baumwurzeln und Stammaufweitungen, insbesondere von größeren Bäumen, mit dem Straßenbelag in Konflikt geraten, was zu einer Verschlechterung der Baumgesundheit und zu Reparaturkosten führt. Ziel dieser Studie war es, (1) allometrische Beziehungen zwischen dem Brusthöhendurchmesser (DBH) und dem Stammfackeldurchmesser (TFD) gängiger städtischer Baumarten herzustellen und (2) Faktoren zu identifizieren, die das Vorhandensein und das Ausmaß von hervorstehenden Wurzeln und auslaufenden Brettwurzeln beeinflussen. Methoden: Die Begriffe "abstehende Wurzeln" und "abstehende Ausbuchtungen" wurden streng definiert als Wurzeln und Ausbuchtungen, die die Grenze zwischen dem offenen Boden und dem angrenzenden Pflaster erreichen oder überschreiten. Im Rahmen der Studie wurden 1.100 Bäume von 14 Arten untersucht, die in Baumgruben in Chai Wan, Hongkong, gepflanzt worden waren. Die Ergebnisse: Der Stammdurchmesser war ein signifikanter Prädiktor für die TFD, war jedoch weniger signifikant, wenn Bäume mit hervorstehenden Wurzeln oder auslaufenden Brettwurzeln separat betrachtet wurden. In den meisten logistischen Modellen stand der DBH in signifikantem und positivem Zusammenhang mit dem Chancenverhältnis des Auftretens von abstehenden Wurzeln und auslaufenden Brettwurzeln. Insgesamt brachte ein Zentimeter mehr DBH eine 1,049- bis 1,114-mal höhere Wahrscheinlichkeit für das Auftreten von hervorstehenden Wurzeln und Ablösungen. Die multiple Regression ergab, dass für jeden Quadratmeter, um den die offene Bodenfläche in den Baumgruben zunahm, die maximale Länge der abstehenden Wurzeln und auslaufenden Brettwurzeln um 0,154 bis 0,172 m zunahm. Um eine genauere Schätzung der überstehenden Wurzeln und auslaufenden Brettwurzeln zu ermöglichen, wurden artspezifische Regressionsergebnisse tabellarisch dargestellt. Schlussfolgerung: Der in dieser Studie empfohlene Ansatz könnte von Stadtplanern und Straßenbauingenieuren zur Optimierung der städtischen Begrünung und der Straßengestaltung verwendet werden.

Resumen. Antecedentes: Los alcorques de árboles son infraestructuras verdes urbanas en áreas pavimentadas. Pero las raíces de los árboles y el collar de las raíces, especialmente de los árboles más grandes, pueden entrar en conflicto con el pavimento, lo

que resulta en la disminución de la salud de los árboles y los costos de reparación. Este estudio tuvo como objetivo (1) establecer relaciones alométricas entre el diámetro a la altura del pecho (DBH) y el diámetro del collar de las raíces (TFD, por sus siglas en inglés) de las especies de árboles urbanos comunes, y (2) identificar los factores que afectan la presencia y la magnitud de las raíces protuberantes. Métodos: Los términos "raíces protuberantes" y "collares sobresalientes" se definieron estrictamente como raíces y collares que alcanzan o exceden el borde entre el suelo abierto y el material de pavimentación adyacente. El estudio encuestó 1100 árboles de 14 especies plantados en alcorques de árboles en Chai Wan, Hong Kong. Resultados: El DBH fue un predictor significativo de TFD, pero fue menos eficiente cuando los árboles con raíces sobresalientes o rebrotes se consideraron por separado. En la mayoría de los modelos logísticos, el DBH se relacionó de manera significativa y positiva con la ratio matemática de la aparición de raíces y brotes sobresalientes. En general, un aumento de centímetros en DBH presentó de 1,049 a 1,114 veces más probabilidad de raíces sobresalientes y collares. La regresión múltiple sugirió que, por cada aumento en metros cuadrados en el área de suelo abierto en el alcorque, la longitud máxima de las raíces sobresalientes y los collares aumentó en 0,154 a 0,172 m. Esta relación podría atribuirse a la asociación subyacente entre DBH y el área de suelo abierto. Los resultados de la regresión específica de la especie se tabularon para permitir una estimación más precisa de las raíces y collares sobresalientes. Conclusión: para los planificadores urbanos y los ingenieros de pavimentos, el enfoque recomendado en este estudio podría adoptarse para optimizar el enverdecimiento urbano y el diseño de pavimentos.